

TU-745
hep-ph/0505252
May, 2005

Reconstructing Dark Matter Density with e^+e^- Linear Collider in Focus-Point Supersymmetry

Takeo Moroi, Yasuhiro Shimizu and Akira Yotsuyanagi

Department of Physics, Tohoku University, Sendai 980-8578, JAPAN

Abstract

It has been known that, in the focus point scenario of supersymmetry, the thermal relic of the lightest superparticle (LSP) is known to be a good candidate of the cold dark matter. Assuming that the LSP in the focus-point scenario be the cold dark matter, we address a question how and how well the relic density of the LSP can be determined once the superparticles are found at future e^+e^- linear collider. We will see that the determinations of the mass of the LSP as well as those of the Higgsino-like chargino and neutralinos, which will be possible by a study of the decay kinematics of the chargino or by threshold scan, will give us important information to theoretically reconstruct the relic density. Once these superparticles become kinematically accessible, relic density of the LSP may be calculated with an accuracy of factor ~ 2 or smaller.

High energy physics and cosmology have had a very important connection for deeper understandings in each field. In particular, progresses in physics at the energy frontier sometimes greatly improved our knowledges on the history of the universe. One of the most famous examples is the big-bang nucleosynthesis [1]; with the understandings of the interactions among the light elements as well as the expansion laws of the universe by general relativity, it became clear that the light nuclei were synthesized in the early universe. Remarkably, nowadays, light-element abundances can be precisely calculated and, for D, ^4He , and ^7Li , theoretical predictions are known to be in reasonable agreements with the observations [2]. As a result, we had an understanding of (some of) the components in the universe. This not only showed a very close connection between high energy physics and cosmology, but also provided a *quantitative* test of the big-bang scenario up to the cosmic temperature of ~ 1 MeV.

Now, we are in a position to have an understanding of physics at the electroweak scale. Although most of the results from the high energy experiments are more or less consistent with the predictions of the standard model of the particle physics, many particle physicists are expecting some new physics at the electroweak scale because of several problems in the standard model, like the naturalness problem, the hierarchy problem, and so on. Among various possibilities, low-energy supersymmetry (SUSY) is the prominent candidate of physics beyond the standard model and hence signals from the superparticles are important target of the future high energy experiments.

If the low-energy SUSY is realized in nature, it will also play important roles in cosmology. In particular, the lightest superparticle (LSP) is known to be a good candidate of the cold dark matter which, although there is no viable candidate within the standard-model particles, is strongly suggested by the present precise observations of the universe. Indeed, recent results from the WMAP suggests the dark matter density parameter to be [3, 4]

$$\Omega_{\text{DM}}^{(\text{WMAP})} h^2 = 0.113_{-0.009}^{+0.008}, \quad (1)$$

where h here is the Hubble constant in units of 100 km/sec/Mpc. In the framework of the low-energy supersymmetry, however, it is not automatic to make the LSP to be the dark matter. In addition, although thermal relic of the LSP is the usual candidate of the dark matter, it has been also pointed out that the LSP dark matter may have non-thermal origin [5]. Thus, once the superparticles are found, it will be important to check if the thermal relic of the LSP is really the dominant component of the cold dark matter; if the theoretically calculated value of the LSP density well agrees with the observed dark-matter density, then it will be an important quantitative confirmation of the (simple) big-bang scenario up to the temperature of ~ 100 GeV.

In order for a precise calculation of the relic density of the LSP, it is necessary to determine the properties of the superparticles by collider experiments. In particular, the relic density is sensitive to the properties of the LSP (such as the mass and couplings), precise determination of those parameters will be necessary. It has been discussed that the high energy e^+e^- linear collider, recently named as the International Linear Collider (ILC), will be a good facility for a detailed study of the superparticles; for various cases, it has been shown that the e^+e^-

linear collider can determine various mass and coupling parameters in the SUSY models very well (see, for example, Refs. [6, 7, 8]). Although, in the current situation, the LHC will probably be the first place where the superparticles will be found, it may not be easy to determine the SUSY parameters accurate enough to precisely calculate the relic density of the LSP [9]. Thus, in the following, we consider how the ILC can help to determine the relic density of the LSP.

Relic density of the LSP depends on how the LSPs annihilate in the early universe when they freeze out from the thermal bath. The dominant annihilation processes of the LSP are model-dependent and there are several parameter regions where the relic density of the LSP becomes consistent with the WMAP value, such as “bulk region,” “coannihilation region,” “rapid-annihilation funnels,” “focus-point region,” and so on [10]. Thus, it is necessary to study the individual cases.

In this letter, we consider one of the cases, the focus-point case; we assume that the dark matter consists of the LSP from the focus-point supersymmetric model, and address a question how and how well we can determine the density parameter of the LSP Ω_{LSP} using the data from the ILC. With reasonable assumptions, we will see that, in the focus point case, relic density of the LSP can be well constrained. Before closing the introduction, we comment on how we proceed our analysis. We assume that the underlying model behind the minimal supersymmetric standard model (MSSM) is the focus point model (with grand unification) and that the dark matter is the thermal relic of the LSP. However, we will propose a procedure to calculate Ω_{LSP} without relying on any high-energy models (such as grand unification, mSUGRA-type parameterization, and so on); our aim is to determine all the relevant *MSSM* parameters from the collider experiments for the calculation of Ω_{LSP} .

We start with a brief review of the focus point scenario. The focus point scenario is characterized by the large (universal) scalar mass at the grand unification theory (GUT) scale [11].^{#1} Although all the squarks and sleptons (as well as the heavier Higgs bosons) acquire multi-TeV masses, naturalness of the electroweak symmetry breaking may be maintained as far as the gauginos and Higgsinos remain relatively light. Thus, in this scenario, gauginos and Higgsinos are the “light” superparticles which may be accessible with the ILC with center-of-mass energy lower than ~ 1 TeV.

Since the important superparticles are the charginos and neutralinos, the relevant parameters for our study are the $U(1)_Y$ and $SU(2)_L$ gaugino masses $m_{\text{G}1}$ and $m_{\text{G}2}$, the supersymmetric Higgs mass μ_H , and the ratio of the vacuum expectation values of two Higgs bosons $\tan \beta$. Properties of the charginos and the neutralinos are determined by these parameters. In particular, the mass matrices of the charginos and the neutralinos are given by^{#2}

$$\mathcal{M}_\pm = \begin{pmatrix} -m_{\text{G}2} & \sqrt{2}g_2 v \cos \beta \\ -\sqrt{2}g_2 v \sin \beta & \mu_H \end{pmatrix}, \quad (2)$$

^{#1}Such a large universal scalar mass may be a result of the “large cut-off supergravity” [12].

^{#2}In fact, the chargino and neutralino masses may acquire radiative corrections, which should be taken into account in the actual study. In the focus point scenario, dominant radiative corrections are from the gauge boson loops and hence are calculable. In our study, we neglect the radiative corrections to the chargino and the neutralino masses.

$$\mathcal{M}_0 = \begin{pmatrix} -m_{G1} & 0 & -g_1 v \cos \beta & g_1 v \sin \beta \\ 0 & -m_{G2} & g_2 v \cos \beta & -g_2 v \sin \beta \\ -g_1 v \cos \beta & g_2 v \cos \beta & 0 & \mu_H \\ g_1 v \sin \beta & -g_2 v \sin \beta & \mu_H & 0 \end{pmatrix}, \quad (3)$$

respectively. Here, g_1 and g_2 are the gauge coupling constants for $U(1)_Y$ and $SU(2)_L$, respectively, and $v \simeq 174$ GeV is the (total) Higgs vacuum expectation value. These mass matrices are diagonalized by the unitary matrices U_{χ^+} , U_{χ^-} , and U_{χ^0} as

$$U_{\chi^+}^T \mathcal{M}_\pm U_{\chi^-} = \text{diag}(m_{\chi_1^\pm}, m_{\chi_2^\pm}), \quad U_{\chi^0}^T \mathcal{M}_0 U_{\chi^0} = \text{diag}(m_{\chi_1^0}, m_{\chi_2^0}, m_{\chi_3^0}, m_{\chi_4^0}). \quad (4)$$

If the GUT relation holds among the gaugino masses, the relation $m_{G2} \simeq 2m_{G1}$ holds (at the electroweak scale) while, for a successful electroweak symmetry breaking, $|\mu_H|$ becomes larger than $|m_{G1}|$. Then, the lightest neutralino, which becomes the LSP, is dominantly Bino although there is sizable contamination of the Higgsino, as we mention below.

It should be noted that Ω_{LSP} is also determined by the previously mentioned four parameters: m_{G1} , m_{G2} , μ_H , and $\tan \beta$. In the focus point scenario, the LSPs dominantly annihilate into the $t\bar{t}$ pair and into the gauge boson pairs ($\chi_1^0 \chi_1^0 \rightarrow W^+ W^-$, $Z^0 Z^0$) when the LSPs freeze out from the thermal bath [13, 9, 14]. These processes are through the Higgsino components in χ_1^0 ; in the focus point scenario, $|\mu_H|$ can be relatively close to m_{G1} and, consequently, sizable contamination of the Higgsino is possible in χ_1^0 . In this case, Ω_{LSP} may become consistent with the WMAP value. In the cosmologically interesting parameter region where $\Omega_{\text{LSP}} \sim 0.1$, $|\mu_H|$ becomes smaller than $|m_{G2}|$ and the lighter chargino χ_1^\pm becomes Higgsino-like while the heavier one χ_2^\pm becomes Wino-like. In addition, in the neutralino sector, χ_1^0 (i.e., the LSP), χ_2^0 , χ_3^0 , and χ_4^0 are Bino-like, Higgsino-like, Higgsino-like, and Wino-like, respectively. As a result, the masses of χ_1^\pm , χ_2^0 , and χ_3^0 are quite degenerate with the approximate relations $m_{\chi_1^0} \sim |m_{G1}|$, $m_{\chi_1^\pm} \sim m_{\chi_2^0} \sim m_{\chi_3^0} \sim |\mu_H|$, and $m_{\chi_2^\pm} \sim m_{\chi_4^0} \sim |m_{G2}|$. These facts will become very important in the following study.

As we mentioned, Ω_{LSP} is determined once the four parameters m_{G1} , m_{G2} , μ_H , and $\tan \beta$ are fixed. With the GUT relation, a narrow strip is obtained on the m_{G2} vs. μ_H plane, where Ω_{LSP} satisfies the WMAP constraint Eq.(1). Such a strip is insensitive to $\tan \beta$ (and the approximate relation $\mu_H \simeq 0.6m_{G2}$ holds on such a strip when $m_{G2} \gtrsim 300$ GeV) [14]. Although our strategy to determine Ω_{LSP} works for most of the points on the strip, (and even for cases without the GUT relation), it will be instructive to see the detail of several cases. Thus, we pick up two parameter points where WMAP value of Ω_{LSP} is realized: Point 1 with relatively small m_{G2} and Point 2 with larger m_{G2} . These points are listed in Table 1; for these points, Ω_{LSP} and the lightest Higgs mass m_h are calculated with adopting that all the sfermion masses are 3 TeV. In the following, several physical quantities such as the cross sections as well as the estimated errors in the reconstructed Ω_{LSP} will be given for these points. (In our numerical analysis, we use the DarkSUSY package [15] to calculate Ω_{LSP} .)

Now we discuss the role of the ILC. As we mentioned, in the focus point case, the chargino(s) and neutralino(s) are the ones which can be produced and studied at the ILC. Thus, we focus on the question what can be measured and studied by the production of the

	Point 1	Point 2
m_{G1}	144 GeV	240 GeV
m_{G2}	300 GeV	500 GeV
μ_H	200 GeV	307 GeV
$\tan \beta$	10	10
$m_{\chi_1^0}$	127 GeV	226 GeV
$m_{\chi_2^0}$	190 GeV	304 GeV
$m_{\chi_3^0}$	208 GeV	311 GeV
$m_{\chi_4^0}$	335 GeV	522 GeV
$m_{\chi_1^\pm}$	176 GeV	291 GeV
$m_{\chi_2^\pm}$	335 GeV	521 GeV
m_h	116 GeV	116 GeV
$\Omega_{\text{LSP}} h^2$	0.113	0.113

Table 1: Points to be used for our analysis.

charginos and the neutralinos.^{#3} For this purpose, we first calculate the production cross sections of the charginos and neutralinos. Since the sleptons are extremely heavy, chargino and neutralino production processes are mediated by the s -channel gauge-boson exchange diagrams; neglecting the selectron diagrams, the chargino and neutralino production cross sections are given by

$$\begin{aligned} \sigma(e^+ e_L^- \rightarrow \chi_X \chi_Y) = & \frac{N_{XY} \beta_f}{8\pi} \left[\left(|C_{LL}|^2 + |C_{LR}|^2 \right) \left(E_X E_Y + \frac{1}{3} |\mathbf{p}_f|^2 \right) \right. \\ & \left. + (C_{LL} C_{LR}^* + C_{LL}^* C_{LR}) m_X m_Y \right], \end{aligned} \quad (5)$$

where E_X , E_Y , and \mathbf{p}_f are the energies of χ_X and χ_Y , and their three-momentum, respectively, $N_{XY} = \frac{1}{2}$ when χ_X and χ_Y are identical and $N_{XY} = 1$ otherwise, and

$$\beta_f^2 = \frac{1}{s^2} \left[s^2 - 2 \left(m_X^2 + m_Y^2 \right) s + \left(m_X^2 - m_Y^2 \right)^2 \right], \quad (6)$$

with \sqrt{s} being the center-of-mass energy of the ILC. Here, the polarization of the electron is specified to be left-handed while the average over the positron polarization is taken. Result for the right-handed electron is given by a similar formula by replacing $C_{LL} \rightarrow C_{RL}$ and $C_{LR} \rightarrow C_{RR}$. For the chargino production,

$$[C_{LL}]_{\chi_X^\pm \chi_Y^\mp} = \frac{e^2}{s} \delta_{XY} + \frac{g_Z^{e_L}}{s - m_Z^2} \left(-\frac{g_2^2}{g_Z} [U_{\chi^-}]_{1X}^* [U_{\chi^-}]_{1Y} + \frac{g_1^2 - g_2^2}{2g_Z} [U_{\chi^-}]_{2X}^* [U_{\chi^-}]_{2Y} \right), \quad (7)$$

^{#3}We assume that the squarks and sleptons will be known to be very heavy by the study of the LHC, and also by the negative searches of these particles at the ILC.

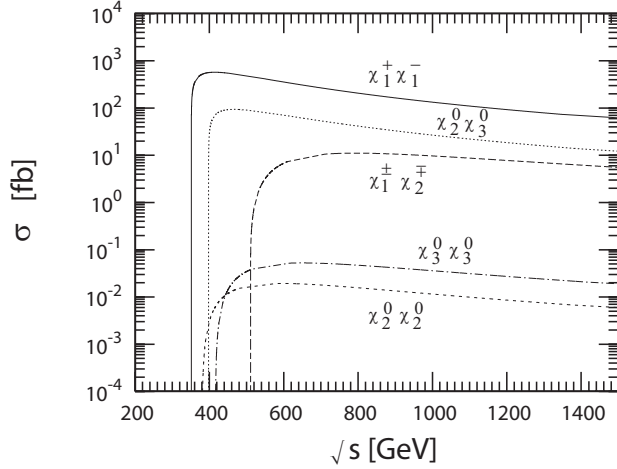


Figure 1: Production cross sections of the charginos and neutralinos for Point 1 for the processes as functions of \sqrt{s} . Here, we have neglected the selectron-exchange diagrams and averaged over the polarization of the electron beam.

where $g_Z^2 \equiv g_1^2 + g_2^2$, and $e = (g_1^{-2} + g_2^{-2})^{-1/2}$ is the electric charge. $[C_{RL}]_{\chi_X^\pm \chi_Y^\mp}$ is obtained by replacing $g_Z^{e_L} \rightarrow g_Z^{e_R}$, where

$$g_Z^{e_L} \equiv \frac{g_1^2 - g_2^2}{2g_Z}, \quad g_Z^{e_R} \equiv \frac{g_1^2}{g_Z}. \quad (8)$$

In addition, $[C_{LR}]_{\chi_X^\pm \chi_Y^\mp}$ and $[C_{RR}]_{\chi_X^\pm \chi_Y^\mp}$ are obtained by the following replacements:

$$[C_{LR}]_{\chi_X^\pm \chi_Y^\mp} = [C_{LL}]_{\chi_X^\pm \chi_Y^\mp} \Big|_{U_{\chi^-} \rightarrow U_{\chi^+}}, \quad [C_{RR}]_{\chi_X^\pm \chi_Y^\mp} = [C_{RL}]_{\chi_X^\pm \chi_Y^\mp} \Big|_{U_{\chi^-} \rightarrow U_{\chi^+}}. \quad (9)$$

For the neutralino production processes,

$$[C_{LL}]_{\chi_X^0 \chi_Y^0} = \frac{g_Z^{e_L} g_Z}{2(s - m_Z^2)} \left([U_{\chi^0}]_{3X}^* [U_{\chi^0}]_{3Y} - [U_{\chi^0}]_{4X}^* [U_{\chi^0}]_{4Y} \right), \quad (10)$$

and $[C_{LR}]_{\chi_X^0 \chi_Y^0} = -[C_{LL}]_{\chi_Y^0 \chi_X^0}$. For the right-polarized electron, the results are obtained by replacing $g_Z^{e_L} \rightarrow g_Z^{e_R}$.

To see the size of the cross sections, we plot the cross sections for various final states in Figs. 1 and 2 for Point 1 and Point 2, respectively, as functions of \sqrt{s} . As one can see, for the processes $e^+e^- \rightarrow \chi_1^+ \chi_1^-$ and $\chi_2^0 \chi_3^0$, cross sections become significantly large (if these processes are kinematically allowed). As we will see, these processes give very important information in calculating the relic density of the LSP.^{#4} On the contrary, cross sections

^{#4}Notice that the chargino χ_1^\pm mostly decays into $W^{\pm(*)} \chi_1^0$ final state (where the superscript * is for virtual particles) while χ_2^0 and χ_3^0 decay into $Z^{0(*)} \chi_1^0$ and $h \chi_1^0$ final states (where h is the lightest Higgs boson). Thus, we expect that some of the chargino and neutralino production events can be distinguished by selecting particular final states. For example, for $e^+e^- \rightarrow \chi_1^+ \chi_1^-$, we can use 1 $l + 2$ jets + missing E_T events, which is not from $\chi_2^0 \chi_3^0$ production, and for $e^+e^- \rightarrow \chi_2^0 \chi_3^0$, 2 $l + 2$ jets + missing E_T events can be used.

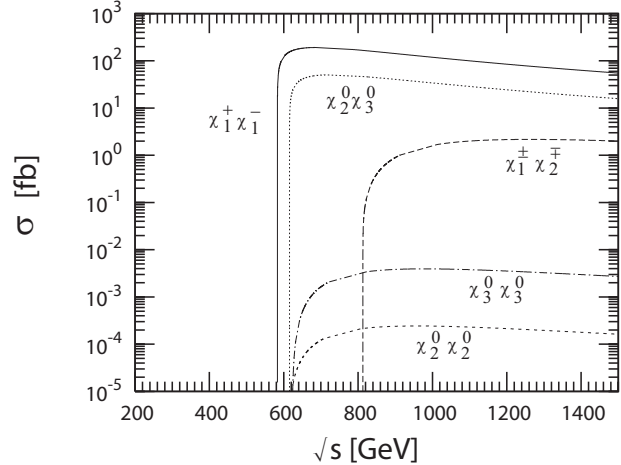


Figure 2: Same as Fig. 1, except for Point 2.

$\sigma(e^+e^- \rightarrow \chi_2^0\chi_2^0)$ and $\sigma(e^+e^- \rightarrow \chi_3^0\chi_3^0)$ are very small. This is due to the facts that the cross sections acquire suppressions from the mixing factors and that these are p -wave processes. Note also that the measurements of the cross sections for $e^+e^- \rightarrow \chi_1^+\chi_1^-$ and $\chi_2^0\chi_3^0$ will tell us that χ_1^\pm , χ_2^0 , and χ_3^0 are Higgsino-like, not Wino-like.

A great advantage of the ILC is that the beam energy can be easily tuned. Thus, it is possible to study various production processes at the threshold region. In particular, in the case of the focus-point scenario, threshold scans of the chargino and neutralino productions give us important information. From the chargino production process $e^+e^- \rightarrow \chi_1^+\chi_1^-$, we can have a precise measurement of the (lighter) chargino mass $m_{\chi_1^\pm}$. Study at the region $\sqrt{s} \sim m_{\chi_2^0} + m_{\chi_3^0}$ is also interesting. At $\sqrt{s} \sim 2|\mu_H|$, three different neutralino production processes become kinematically allowed since the masses of χ_2^0 and χ_3^0 are close. However, the cross sections for $e^+e^- \rightarrow \chi_2^0\chi_2^0$ and $e^+e^- \rightarrow \chi_3^0\chi_3^0$ are very small in particular at the threshold region since these processes are p -wave suppressed; we can see that the cross sections for these processes are much smaller than $\sigma(e^+e^- \rightarrow \chi_2^0\chi_3^0)$. Thus, we observe only the process $e^+e^- \rightarrow \chi_2^0\chi_3^0$. Since the process $e^+e^- \rightarrow \chi_2^0\chi_3^0$ becomes kinematically allowed when $\sqrt{s} = m_{\chi_2^0} + m_{\chi_3^0}$, we can determine the combination $m_{\chi_2^0} + m_{\chi_3^0}$ or, equivalently, the averaged mass of χ_2^0 and χ_3^0 :

$$\bar{m}_{\chi_{23}^0} \equiv \frac{1}{2} (m_{\chi_2^0} + m_{\chi_3^0}), \quad (11)$$

by the scan around $\sqrt{s} \sim m_{\chi_2^0} + m_{\chi_3^0}$.

In order to study the properties of the LSP, on the contrary, \sqrt{s} should better be optimized so that the production of the lighter chargino, which decays into the LSP χ_1^0 , is enhanced. Once the charginos are copiously produced, then the mass of the LSP (more precisely, the mass difference $m_{\chi_1^\pm} - m_{\chi_1^0}$) is determined by the study of the energy distribution

of the decay products.^{#5}

At the ILC, errors in the measurements of $m_{\chi_1^\pm}$, $\bar{m}_{\chi_{23}^0}$, and $m_{\chi_1^0}$ are expected to be mostly from the detector resolutions [8]. For example, it was pointed out that, for some choice of the SUSY parameters, masses of the charginos can be determined using e^+e^- colliders with the errors of ~ 50 MeV by the threshold scan. In addition, from the energy distribution of the decay products of the chargino and neutralinos, the mass of the LSP is also determined with the uncertainty of ~ 50 MeV. Although these results are for the case of Wino-like chargino and neutralino, we expect that three mass parameters (i.e., $m_{\chi_1^\pm}$, $m_{\chi_1^0}$, and $\bar{m}_{\chi_{23}^0}$) are accurately measured once χ_1^\pm , χ_2^0 , and χ_3^0 become kinematically accessible at the ILC. Since χ_1^0 is Bino-like while χ_1^\pm (as well as χ_2^0 and χ_3^0) are Higgsino-like, we can constrain m_{G1} and μ_H from the measurements of $m_{\chi_1^0}$ and $m_{\chi_1^\pm}$ (or from the masses of other Higgsino-like neutralinos). In addition, the “mass difference” $\bar{m}_{\chi_{23}^0} - m_{\chi_1^\pm}$ is sensitive to some combination of $\tan\beta$ and m_{G2} .

Although the relic density of the LSP depends on four MSSM parameters (m_{G1} , m_{G2} , μ_H , and $\tan\beta$), interesting bound on Ω_{LSP} can be obtained even at this stage. To see this, we can perform the following analysis. Let us imagine a situation where $m_{\chi_1^\pm}$, $m_{\chi_1^0}$, and $\bar{m}_{\chi_{23}^0}$ are well measured at the ILC. Using these quantities, we impose three constraints on the four underlying parameters and determine m_{G1} , μ_H , and $\tan\beta$ as functions of m_{G2} . In the determination of m_{G1} and μ_H , in fact, there are four possible choices of their signs: $(\text{sign}(m_{G1}), \text{sign}(\mu_H)) = (+, +), (+, -), (-, +)$, and $(-, -)$.^{#6} Effects of the signs of μ_H and m_{G1} are quite different. In order to see how the reconstructed relic density depends on m_{G2} and $\text{sign}(\mu_H)$, here let us consider the case where the sign of the reconstructed m_{G1} is the same as that of the underlying one; effects of $\text{sign}(m_{G1})$ will be discussed later. Once we reconstruct m_{G1} , μ_H , and $\tan\beta$, we calculate the relic density of the LSP as a function of m_{G2} , which we call

$$\hat{\Omega}_{\text{LSP}}(m_{G2}; m_{\chi_1^\pm}, m_{\chi_1^0}, \bar{m}_{\chi_{23}^0}).$$

In Figs. 3 and 4, we plot $\hat{\Omega}_{\text{LSP}}(m_{G2}; m_{\chi_1^\pm}, m_{\chi_1^0}, \bar{m}_{\chi_{23}^0})$ as a function of m_{G2} , with $m_{\chi_1^\pm}$, $m_{\chi_1^0}$, and $\bar{m}_{\chi_{23}^0}$ being fixed to be the values from Point 1 and Point 2, respectively. We use a fixed value of the lightest Higgs boson mass m_h . (We have checked that $\hat{\Omega}_{\text{LSP}}$ is insensitive to the change of m_h .) The lines have endpoints; this is due to the fact that, when m_{G2} becomes too large or too small, there is no value of $\tan\beta$ which consistently reproduces the observed mass spectrum. To demonstrate this, we also showed the points where $\tan\beta$ takes several specific values. In the figures, the results for the cases with positive and negative μ_H are shown. As one can see, the line for the $\mu_H < 0$ case is “attached” to one of the endpoints of

^{#5}From the $\chi_2^0\chi_3^0$ production, we may in principle perform a similar analysis to determine the mass of the LSP. In this case, however, error may become larger because the masses of χ_2^0 and χ_3^0 differ by $O(1)$ GeV. Global fit using all the data should be appropriate once the charginos and neutralinos are really found in the future.

^{#6}To be more precise, these signs are the relative signs between m_{G1} and m_{G2} or μ_H and m_{G2} . We assume that the gaugino masses and μ_H are real in order to avoid constraints from CP violations.

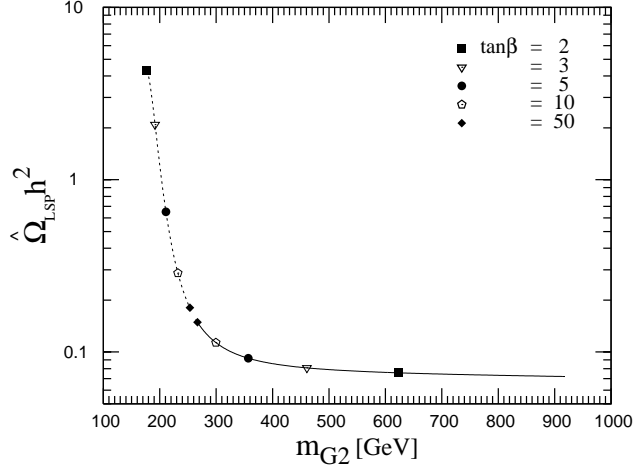


Figure 3: $\hat{\Omega}_{\text{LSP}}(m_{\text{G2}}; m_{\chi_1^\pm}, m_{\chi_1^0}, \bar{m}_{\chi_{23}^0})$ as a function of m_{G2} , where $m_{\chi_1^\pm}$, $m_{\chi_1^0}$, and $\bar{m}_{\chi_{23}^0}$ are fixed by the underlying values for Point 1 with positive μ_H (solid) and negative μ_H (dashed). Marks on the figure indicate the points with $\tan\beta = 2, 3, 5, 10, 50$.

the line for $\mu_H > 0$. This is from the fact that, at the tree level, flip of sign(μ_H) is equivalent to the change $\beta \rightarrow \pi - \beta$.

As one can see, the case with negative μ_H may give large uncertainty in the reconstructed Ω_{LSP} . If $\mu_H < 0$, however, smaller m_{G2} is required than in the case of positive- μ_H in order to reproduce the observed mass spectrum, as shown in the figures. Then, $m_{\chi_2^\pm}$, for example, may become smaller than the experimental bound from the negative search for the $\chi_1^\pm \chi_2^\mp$ production process. For Point 1 (Point 2), $\sqrt{s} \gtrsim 480$ GeV (750 GeV) is enough to exclude the $\mu_H < 0$ case. Thus, in the following, we assume that this is the case and neglect the uncertainty from the $\mu_H < 0$ case. Then, even without any further constraint on m_{G2} , relic density of the LSP can be determined within a factor of ~ 2 or smaller.

For a quantitative study of the uncertainties in the reconstructed LSP density, we define the following quantity:

$$D_{m_I} \equiv \left| \frac{\partial \ln \hat{\Omega}_{\text{LSP}}}{\partial \ln m_I} \right|, \quad m_I = m_{\chi_1^\pm}, m_{\chi_1^0}, \bar{m}_{\chi_{23}^0}, m_{\text{G2}}, \quad (12)$$

so that^{#7}

$$\frac{\delta \hat{\Omega}_{\text{LSP}}}{\hat{\Omega}_{\text{LSP}}} = \left[\left(D_{m_{\chi_1^\pm}} \frac{\delta m_{\chi_1^\pm}}{m_{\chi_1^\pm}} \right)^2 + \left(D_{m_{\chi_1^0}} \frac{\delta m_{\chi_1^0}}{m_{\chi_1^0}} \right)^2 + \left(D_{\bar{m}_{\chi_{23}^0}} \frac{\delta \bar{m}_{\chi_{23}^0}}{\bar{m}_{\chi_{23}^0}} \right)^2 + \left(D_{m_{\text{G2}}} \frac{\delta m_{\text{G2}}}{m_{\text{G2}}} \right)^2 \right]^{1/2}. \quad (13)$$

For Point 1 and Point 2, we found $(D_{m_{\chi_1^\pm}}, D_{m_{\chi_1^0}}, D_{\bar{m}_{\chi_{23}^0}}, D_{m_{\text{G2}}})$ to be $(19, 8.1, 8.6, 1.5)$ and $(7.5, 7.9, 8.5, \sim 0.01)$, respectively. (Here, notice that $D_{m_{\text{G2}}}$ for Point 2 is accidentally small

^{#7}In fact, some of the observables may be correlated (in particular because, as we mentioned, one of the observable would be $m_{\chi_1^\pm} - m_{\chi_1^0}$, not $m_{\chi_1^0}$). Here, we neglect effects of such correlations.

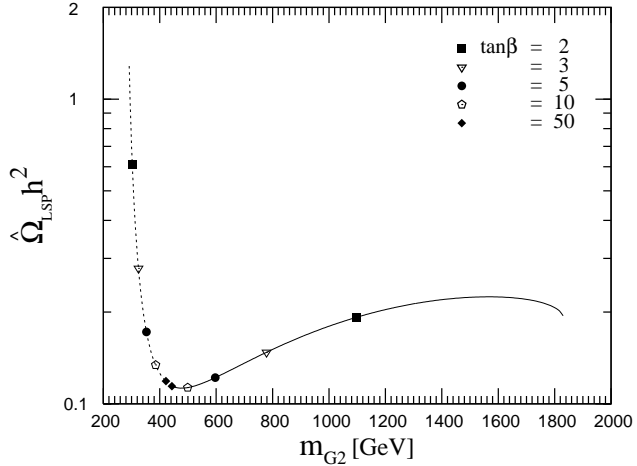


Figure 4: Same as Fig. 3, except for Point 2.

because of the choice of the underlying parameters.) As we mentioned, at the ILC, $m_{\chi_1^\pm}$, $m_{\chi_1^0}$, and $\bar{m}_{\chi_{23}^0}$ will be well determined with the error of 0.1 % or less [8] (although the errors should depend on the model parameters). Using the values of $D_{m_{\chi_1^\pm}}$, $D_{m_{\chi_1^0}}$, and $D_{\bar{m}_{\chi_{23}^0}}$ given above, $\delta\hat{\Omega}_{\text{LSP}}$ from $\delta m_{\chi_1^\pm}$, $\delta m_{\chi_1^0}$, and $\delta\bar{m}_{\chi_{23}^0}$ is very small.

For a better determination of Ω_{LSP} , some information about m_{G2} is necessary. For example, if we try to determine Ω_{LSP} with ~ 10 % accuracy, which is the level of the WMAP value, m_{G2} should be determined within the uncertainty of ~ 30 GeV for Point 1 and ~ 170 GeV for Point 2. If we impose the GUT relation among the gaugino masses, m_{G2} is accurately determined. However, we do not pursue this direction since we hope to calculate Ω_{LSP} in the framework of the MSSM.

The $SU(2)_L$ gaugino mass m_{G2} is approximately equal to the masses of χ_2^\pm and χ_4^0 . Thus, if we know something about $m_{\chi_2^\pm}$ or about $m_{\chi_4^0}$, it will help us to set a bound on m_{G2} . Some constraint may be given by the LHC. Even in the focus-point scenario, a sizable amount of the gluino may be produced at the LHC, and some of them decay into χ_2^\pm or χ_4^0 (and other quark jets). These charginos and neutralinos will decay by emitting W^\pm or Z^0 boson (or the lightest Higgs boson, in some case). If the gauge bosons subsequently decay into the leptons, for example, we may have events with multi-leptons and missing E_{T} , whose background is probably relatively small. By studying the energy distribution of the charged leptons, some information about the Wino-like particles may be obtained.

If χ_2^\pm or χ_4^0 becomes kinematically accessible at the ILC, some direct information of these particles will become available. For example, we can look for the associated production processes of these Wino-like particles with lighter charginos or neutralinos (although the cross sections for the associated productions are relatively suppressed). For example, with large enough \sqrt{s} , cross section for the $\chi_1^\pm\chi_2^\mp$ production process is sizable, as shown in Figs. 1 and 2. With the threshold scan of this process, $m_{\chi_2^\pm}$ may be measured, resulting in a good determination of m_{G2} .

In order to constrain m_{G2} , we may also use $\tan\beta$ dependence of the lightest Higgs mass. As shown in Figs. 3 and 4, the reconstructed value of $\tan\beta$ depends on m_{G2} . Importantly, smaller value of $\tan\beta$ results in more suppressed value of the lightest Higgs mass. Although the lightest Higgs mass depends on other MSSM parameters (in particular, on the stop masses [16]), too small $\tan\beta$ will be excluded by the detailed study of the lightest Higgs, which will be possible at the ILC [6, 7, 8]. If we obtain a lower bound on $\tan\beta$ from the measurement of the Higgs mass, it will also help to determine the relic density of the LSP.

Another possibility to constrain m_{G2} is to measure the cross sections for the processes $e^+e^- \rightarrow \chi_1^0\chi_2^0$ and $e^+e^- \rightarrow \chi_1^0\chi_3^0$. In some case, χ_2^0 and χ_3^0 both dominantly decay into $Z^{0(*)}\chi_1^0$. If so, the $\chi_1^0\chi_2^0$ and $\chi_1^0\chi_3^0$ production processes has the final state with 2 l + missing E_T and 2 jets + missing E_T . It may not be easy to distinguish these two events, but we can just consider the total cross section $\sigma(e^+e^- \rightarrow \chi_1^0\chi_2^0) + \sigma(e^+e^- \rightarrow \chi_1^0\chi_3^0)$. For Point 2, for example, the total cross section $\sigma(e^+e^- \rightarrow \chi_1^0\chi_2^0) + \sigma(e^+e^- \rightarrow \chi_1^0\chi_3^0)$ monotonically increases as a function of m_{G2} from 15 fb (for $m_{G2} = 440$ GeV) to 29 fb (for $m_{G2} = 1830$ GeV). Thus, if this cross section is precisely measured, we can obtain another information about m_{G2} . However, it should be noted that several serious standard-model backgrounds may exist. In particular, the processes $e^+e^- \rightarrow W^+W^-$, $\nu_e\bar{\nu}_e Z^0$, and $W^+W^-Z^0$ have large cross sections. (For $\sqrt{s} = 1$ TeV, $\sigma(e^+e^- \rightarrow W^+W^-) \sim 3$ pb, $\sigma(e^+e^- \rightarrow \nu_e\bar{\nu}_e Z^0) \sim 900$ fb, and $\sigma(e^+e^- \rightarrow W^+W^-Z^0) \sim 60$ fb for the unpolarized electron beam [17].) Although these processes are suppressed for the right-polarized electron beam, cross sections for these processes are much larger than $\sigma(e^+e^- \rightarrow \chi_1^0\chi_2^0) + \sigma(e^+e^- \rightarrow \chi_1^0\chi_3^0)$. Thus, some appropriate kinematical cuts should be necessary to use these modes for the determination of $\sigma(e^+e^- \rightarrow \chi_1^0\chi_2^0) + \sigma(e^+e^- \rightarrow \chi_1^0\chi_3^0)$.

So far, we have not considered effects of the sign of m_{G1} . Unfortunately, Ω_{LSP} depends on the sign of m_{G1} although the determination of $\text{sign}(m_{G1})$ seems challenging. For the case with negative m_{G1} , $\Omega_{\text{LSP}}h^2$ varies from 0.9 to 7.4 (Point 1) and from 0.2 to 6.7 (Point 2). If $\text{sign}(m_{G1})$ is undetermined, thus, two-fold ambiguity will remain. However, experimental determination of $\text{sign}(m_{G1})$ may be possible [18]. In addition, if the GUT relation among the (absolute values of) gaugino masses is experimentally confirmed, it will give another hint of the signs of the gaugino masses.

We have not discussed possible errors of Ω_{LSP} originating from parameters other than $m_{\chi_1^\pm}$, $m_{\chi_1^0}$, and $\bar{m}_{\chi_{23}^0}$, and m_{G2} . Theoretical prediction on Ω_{LSP} , in fact, depends also on other parameters. For the process $\chi_1^0\chi_1^0 \rightarrow t\bar{t}$, which can be the dominant pair annihilation process of the LSP, there exists the t channel stop exchange diagram, so the cross section for this process depends on the stop masses. Since the stops are very heavy in the focus point scenario, the stop masses will not be directly measured at the ILC. In addition, the cross section for this process also depends on the lightest Higgs boson mass through the s -channel exchange of the Higgs boson. (Of course, the lightest Higgs boson mass will be accurately measured at the ILC, so the latter diagram will not give serious uncertainty.) However, the process $\chi_1^0\chi_1^0 \rightarrow t\bar{t}$ is dominated by the s -channel Z^0 exchange diagram [9]. We have checked that the reconstructed value of Ω_{LSP} is insensitive to the choice of the stop mass and m_h . Other possible uncertainty may be from the pair annihilation into the $b\bar{b}$ final state, which

may give $\sim 10\%$ contribution to the total annihilation cross section when $\tan\beta$ is very as large as ~ 50 because of the enhanced bottom-quark Yukawa coupling [9]. The cross section for the process $\chi_1^0\chi_1^0 \rightarrow b\bar{b}$ cannot be calculated unless we know the pseudo-scalar Higgs boson mass. Thus, $\sim 10\%$ uncertainty may remain unless the pseudo-scalar Higgs boson mass is somehow constrained. Uncertainties from the first and second generation sfermions are irrelevant since the pair annihilation into light fermions is p -wave suppressed.

In this letter, we have seen that, if the dominant component of the cold dark matter is the thermal relics of the LSP in the focus-point supersymmetric model, we will have a good chance to theoretically reconstruct the cold dark matter density once the superparticles becomes kinematically accessible at the ILC. Positive confirmation of the dark matter density will give us a quantitative understanding of our universe up to the temperature around 100 GeV. Of course, even in the framework of the supersymmetric models, there are several possibilities to realize the LSP dark matter. Superparticle spectrum and the observables at the collider experiments depend on the model. Thus, for other cases, it is also necessary to study how and how well we can reconstruct the dark matter density. In addition, in our study, we have not performed detailed detector simulations to have accurate errors in the observables (although we have seen that, using the reasonable estimate of the errors, determination of Ω_{LSP} seems promising with a good accuracy). We leave these for future studies.

Note added: While finalizing this letter, we found the paper [19] which may have some relevance with our analysis.

Acknowledgment: This work is supported in part by the 21st century COE program, “Exploring New Science by Bridging Particle-Matter Hierarchy.” The work of T.M. is also supported by the Grants-in Aid of the Ministry of Education, Science, Sports, and Culture of Japan No. 15540247.

References

- [1] G. Gamow, Phys. Rev. **70** (1946) 572; R. A. Alpher, H. Bethe, and G. Gamow, Phys. Rev. **73** (1948) 803.
- [2] For review, see, for example, B. D. Fields and S. Sarkar, Phys. Lett. B **592** (2004) 202.
- [3] C. L. Bennett *et al.*, Astrophys. J. Suppl. **148** (2003) 1.
- [4] S. Eidelman *et al.* [Particle Data Group], Phys. Lett. B **592** (2004) 1.
- [5] T. Moroi and L. Randall, Nucl. Phys. B **570** (2000) 455; M. Fujii and K. Hamaguchi, Phys. Rev. D **66** (2002) 083501.
- [6] S. Matsumoto *et al.* [JLC Group], “JLC-1,” KEK Report 92-16 (1992).
- [7] S. Kuhlman *et al.* [The NLC ZDR Design Group and The NLC Physics Working Group], “Physics and Technology of the Next Linear Collider,” BNL 52-502 (1996).

- [8] J. A. Aguilar-Saavedra *et al.* [ECFA/DESY LC Physics Working Group], arXiv:hep-ph/0106315.
- [9] B. C. Allanach, G. Belanger, F. Boudjema and A. Pukhov, JHEP **0412** (2004) 020.
- [10] J. R. Ellis, K. A. Olive, Y. Santoso and V. C. Spanos, Phys. Lett. B **565** (2003) 176; H. Baer and C. Balazs, JCAP **0305** (2003) 006; [arXiv:hep-ph/0303114]. U. Chattopadhyay, A. Corsetti and P. Nath, Phys. Rev. D **68** (2003) 035005.
- [11] J. L. Feng and T. Moroi, Phys. Rev. D **61** (2000) 095004; J. L. Feng, K. T. Matchev and T. Moroi, Phys. Rev. Lett. **84** (2000) 2322; Phys. Rev. D **61** (2000) 075005.
- [12] M. Ibe, K. I. Izawa and T. Yanagida, Phys. Rev. D **71** (2005) 035005.
- [13] J. L. Feng, K. T. Matchev and F. Wilczek, Phys. Lett. B **482** (2000) 388.
- [14] M. Ibe, T. Moroi and T. Yanagida, arXiv:hep-ph/0502074.
- [15] P. Gondolo *et al.*, JCAP **0407** (2004) 008.
- [16] Y. Okada, M. Yamaguchi and T. Yanagida, Prog. Theor. Phys. **85** (1991) 1; H. E. Haber and R. Hempfling, Phys. Rev. Lett. **66** (1991) 1815; J. R. Ellis, G. Ridolfi and F. Zwirner, Phys. Lett. B **257** (1991) 83.
- [17] H. Murayama, Ph. D. Thesis (UT-580).
- [18] S. Y. Choi, J. Kalinowski, G. Moortgat-Pick and P. M. Zerwas, Eur. Phys. J. C **22** (2001) 563 [Addendum-ibid. C **23** (2002) 769].
- [19] H. Baer, A. Mustafayev, E.-K. Park and S. Profumo, arXiv:hep-ph/0505227.